Article

Journal of Vibration and Control
19(13) 1962–1979

DOI: 10.1177/1077546312449643
jvc.sagepub.com

Suppression of vibration caused by residual unbalance of rotor for magnetically suspended flywheel

Jiqiang Tang[1,2], Bin Liu[3], Jiancheng Fang[4] and Shuzhi Sam Ge[2]

Abstract

For a magnetically suspended flywheel (MSFW), the residual unbalance of rotor can cause synchronous vibration and reduce the attitude control precision of spacecrafts. To eliminate the vibration caused by the residual unbalance of rotor suspended by magnetic bearing, the theorem of unbalance vibration is researched, and it is pointed out that the vibration can be successfully suppressed through the elimination of synchronous component in magnetic suspension forces by a magnetic suspension force compensation method. Based on the general notch filter, this method is proposed to be closed-loop style when the rotor rotates beyond its critical stable speed and to be open-loop style when the speed of the rotor is less than the critical stable speed by additional displacement stiffness compensation segment, open and closed-loop control method. The stability of this method is analyzed and the ability to eliminate n octave synchronous is verified in the whole speed range of the rotor. Experimental results demonstrate that this method can suppress the unbalance vibration significantly in the operation speeds of MSFW and is suitable for MSFW in that the rotor traverses its critical stable speed frequently.

Keywords

Magnetic bearing, magnetically suspended flywheel (MSF), notch filter, residual unbalance, vibration

Received: 26 January 2012; accepted: 17 April 2012

1. Introduction

Flywheel is an inertial actuator in a spacecraft attitude control system and is used to generate suitable attitude control torques for correcting spacecraft attitude deviation or adjusting to an assigned attitude. Flywheels used as inertial actuators can be divided into reaction flywheels and momentum flywheels, and generate attitude torque by changing their rotor's speed to keep the spacecraft stable or change its attitude through momentum exchange with spacecraft (Kenny et al., 2005; Tang and Chen, 2009). Several investigators have claimed (Song et al., 2007; Wang and Hu, 2009) that disturbances produced by, for example, friction, residual unbalance of rotor, and so on can induce error between torque command and actual output torque, and furthermore cause additional disturbance to satellite attitude control system. Compared with conventional ball bearing flywheels, an MSFW has no mechanical contact between rotor and stator since there is a prescribed gap, and MSFWs have some general advantages such as higher speed, no mechanical contacts, no lubrication, and no stiction, etc (Yin et al., 2007). Within this gap the rotor can move in all three

[1]School of Instrument Science and Opto-electronics Engineering, Beihang University, China
[2]Department of Electrical and Computer Engineering, National University of Singapore, Singapore
[3]School of Automation Science and Electrical Engineering, Beihang University, China
[4]School of Instrument Science and Opto-electronics Engineering, Beihang University, China

Corresponding author:
Jiqiang Tang, School of Instrument Science and Opto-electronics Engineering, Beihang University, 100191, China
Email: tjq_72@163.com

translational directions and rotate in all three rotational directions. If the magnetic bearing position control loops are equipped with a highly effective active vibration control law, the vibrations of the wheel can be isolated from the spacecraft, which will improve the stability of attitude control and point accuracy of the satellite greatly.

The sources causing the vibration of the wheel include interior disturbance and exterior disturbance. Interior noise, residual unbalance disturbance, biased force of motor and anisotropy of magnetic bearing force are regarded as interior disturbance. Liu et al. (2010) pointed out that the exterior disturbance includes rotation of spacecraft, exterior noise and so on. All disturbances may cause the synchronous vibration, low frequency movement and random disturbance of the wheel. In particular, the synchronous vibration is caused mostly by residual unbalance disturbance, biased force of motor, anisotropy of magnetic bearing force and non-uniformity of material. With respect to MSFW, the magnetic suspension force is strongly nonlinear, the magnetic suspension force linearization method is adding an additional biased magnetic field to the magnetic bearing generally. Therefore the magnetic suspension force is limited not only to the current of the coil (e.g. current stiffness), but also to the length of the gap of the magnetic bearing (e.g. displacement stiffness). Even if the detecting errors of sensors can be eliminated completely by a filtering method, the gap change of the magnetic bearing still makes the magnetic suspension force fluctuate.

In order to reduce the disturbance, the unbalance magnetic tension caused by negative stiffness of the magnetic bearings should be compensated. Ali, Jerome and Saito et al. (1996, 2006) presented a disturbance feedback control method to compensate harmonious vibration of different orders, but this method increased the complexity of the control system. Other linearization methods presented by Peng et al. (2006) perhaps can avoid the unbalance tension caused by the biased magnetic field, but they cause additional complex problems such as the nonlinearity of electromagnetic force.

In term of the effects of active controlling vibration, the vibration control method may be classified into three categories by Takeshi (2001), Bi et al. (2005) and Peng et al. (2006): zero displacement, zero current and zero magnetic force. With respect to MSFW, our control aim is to make the rotor rotate around its inertial axis, so this method is classified into zero magnetic force vibration control category. For the zero magnetic force vibration control method, there are two means: the first ones presented by Johannes et al.(2000) is based on state observer, which generally requires an accurate system model, and its effectiveness relies mostly on the model error; the second ones presented by several investigators (Li and Tadahiko, 2003; Li et al., 2002; Zhang and Tadahiko, 2004) are based on the notch filter method to research the magnetic bearing with a single plane and merely overcome the control problem of rotor rotating around it centroid in X direction and/or Y direction. The unbalance vibration of the rotor can provoke the fundamental frequency disturbance of MSFW, as it is the main vibration source for MSFW.

For MSFW with active reluctance-force-type magnetic bearing, its schematic of magnetic bearing-rotor system with residual unbalance and the real reason of the vibration caused by residual unbalance of the rotor are presented, and the self-alignment ability of a high-speed rotor has been proved. By means of the active control of the magnetic bearing, the idea of making a high-speed rotor rotate around its inertial axis to reduce its vibration is presented first. The presented magnetic bearing-rotor system mode, which is distinguished from existing models, regards the disturbance caused by residual unbalance of the rotor as the interior factor of the magnetic bearing. Because magnetic force is composed of current stiffness component and displacement stiffness component, the real reason that existing control methods which aim to eliminate synchronous component in the current of the magnetic bearing cannot eliminate the vibration caused by residual unbalance of rotor completely is found in this paper, i.e. the displacement component of disturbance in the magnetic force still exists. Considering not only static unbalance but also dynamic unbalance of the rotor, the displacement relationship between the geometric center and the centroid of the rotor is presented, linearized, and the dynamic equation group of the magnetic bearing-rotor system with the rotor's static and dynamic unbalance is identified. The compensation method of synchronous component in displacement stiffness proposed by us is adding an additional current, which is equal in magnitude and opposite in direction to the synchronous component, to counteract the synchronous component in the displacement stiffness. To realize this vibration suppression method, magnetic suspension force based on synchronous component, new methods of vibration parameter identification and magnetic suspension force compensation are presented. This vibration suppression method is stable and able to eliminate n octave synchronous vibration of the rotor in the whole speed range of the rotor. Experimental results demonstrate that this method is fit for MSFW in that its rotor frequently traverses the critical stable speed.

2. Theory of unbalance vibration for the magnetic bearing-rotor system

2.1. *Essence of the vibration caused by residual unbalance of rotor*

The MSFW with 50 Nms angular momentum, as shown in Figure 1, consists of rotor and stator. The stator is formed by a shaft, two axial magnetic bearings (A and B), two position sensors (A and B), two radial magnetic bearings (A and B) and one motor. The stator is mounted on the base and the housing is used to provide the vacuum circumstance about less than 2 Pa to avoid the viscous air drag when the rotor rotates at high speed.

Other than the rotation around the axial axis driven by a motor, the other 5 degrees-of-freedom (d.f.) of the rotor are controlled by magnetic bearings. Axial magnetic bearing-A and B control the translation of the rotor along the axial axis, radial magnetic bearing-A and B located on the upper and lower side of the rotor control the translation and rotation of the rotor about two radial axes. Position sensor-A and B are integrated axial/radial eddy current sensors, the displacements and tilting angles of the rotor are measured by them. Touchdown bearings as auxiliary equipments not shown in Figure 1 are used to support the rotor when the magnetic bearings are turned off or fail.

To simplify the question, it is assumed that:

(i) The rotor is an axle symmetrical rigid rotor
(ii) When the rotor is steady, the magnetic force acting on the rotor in direction of x axle or y axle individually is orthogonal and independent of each other
(iii) Couple between axial magnetic bearings and radial magnetic bearings does not exist
(iv) Axial translation of the rotor is not considered.

A schematic diagram of a magnetic bearing-rotor system with residual unbalance is shown in Figure 2. Denoting the geometric center of the rotor by O_G, the centroid of the rotor by O_m, then O_G does not coincide with O_m due to the residual unbalance, there is an angle between geometric axis and inertial axis of the rotor. Denote the central plane of magnetic bearing-A by Π_1, the central plane of magnetic bearing- B by Π_2, and the central plane of rotor by Π, respectively.

Let C_1 stand for the point of intersection of the inertia axis and the central plane of magnetic bearing-A(Π_1), C_2 the point of intersection of the inertial axis and the central plane of magnetic bearing-B(Π_2). O_1 the point of intersection of the geometric axis and the central plane of magnetic bearing-A (Π_1), O_2 the point of intersection of the geometric axis and central plane of magnetic bearing-B (Π_2), N the point of intersection of central plane of rotor (Π) and the beeline through two centers of magnetic bearing-A and B, O the point of intersection of central plane of rotor (Π) and inertial axis of rotor.

Let AX, AY present the direction of X axis or Y axis for magnetic bearing-A, respectively. Let BX, BY present the direction of X axis or Y axis for magnetic bearing-B, respectively. When the rotor suspended rigidly rotates at a given angular speed ω_R, whose velocity and phase are obtained from an optic-electric encoder or an array of hall sensors of the driving motor for flywheel, the relationship among O_G, O_m and O of the rotor in its central plane is shown in Figure 3. Set O as the origin of the revolving coordinate

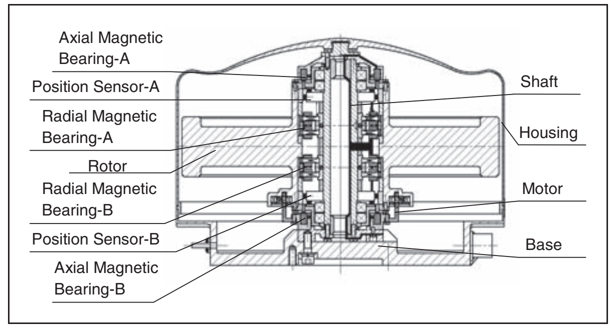

Figure 1. Structure diagram of a magnetically suspended flywheel.

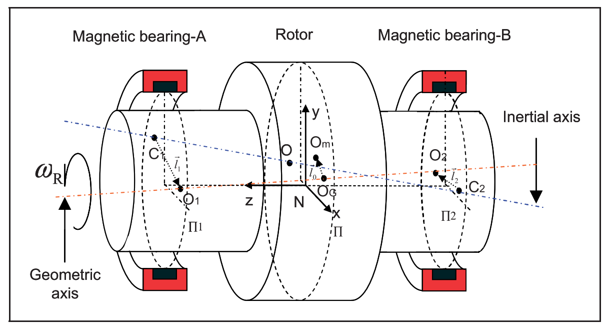

Figure 2. Schematic diagram of magnetic suspension of rotor with residual unbalance.

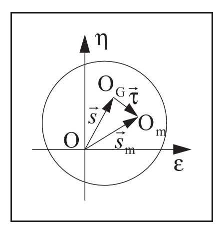

Figure 3. Relationship among O_G, O_m and O of rotor.

of $o\varepsilon\eta$ at the central plane Π of the rotor, and then the geometric center O_G of the rotor deviates from O with vectorial distance $\vec{s}$. Given that O_G does not coincide with O_m and the vectorial distance is $\vec{\tau}$.

So the vectorial distance $\vec{s}_m$ of centroid O_m deviating from O is

$$\vec{s}_m = \vec{s} + \vec{\tau} \tag{1}$$

If only the elastic restoring force described as ks acts on the rotor without any damping force, then the movement equation of the rotor is obtained according to Newton second law

$$m\ddot{\vec{s}}_m + ks = 0 \tag{2}$$

where m is the mass of rotor.

When the revolving coordinate $o\varepsilon\eta$ rotates at the speed of ω around the inertial axis of the rotor, then $\vec{s}$ can be given by $\vec{s} = \lambda e^{i\omega t}$, $\vec{\tau}$ can be given by $\vec{\tau} = \delta e^{i\omega t}$, where λ is the module of $\vec{s}$, and δ the module of $\vec{\tau}$.

So $\ddot{s}_m = \ddot{\lambda} e^{i\omega t} + 2\dot{\lambda} e^{i\omega t} - \lambda e^{i\omega t} \cdot \omega^2 - \delta e^{i\omega t} \cdot \omega^2$

Define $\omega_k = \sqrt{k/m}$, then we have

$$\ddot{\lambda} + 2i\omega\dot{\lambda} + (\omega_k^2 - \omega^2)\lambda = \delta\omega^2 \tag{3}$$

The solution of (3) can be expressed as

$$\lambda = c_1 e^{i(\omega_k - \omega)t} + c_2 e^{-i(\omega_k + \omega)t} + \delta\omega^2/(\omega_k^2 - \omega^2) \tag{4}$$

So the amplitude of the vibration of the geometric center for the rotor without damping is $|s| = \lambda\omega^2/(\omega_k^2 - \omega^2)$.

Then amplitude of the vibration for the centroid of rotor without damping is

$$|s_m| = \lambda\omega^2/(\omega_k^2 - \omega^2) + \lambda = \lambda\omega_k^2/(\omega_k^2 - \omega^2) \tag{5}$$

When $\omega \gg \omega_k$, then $|\vec{s}| \to \lambda$, $|\vec{s}_m| \to 0$, that is to say the rotor tends to rotate around its own centroid with the increase in its speed. Namely, the high-speed rotor has the ability of self-alignment.

But the work principle of active reluctance-force-type magnetic bearing is that the position sensor measures the displacement of rotor from its reference position, a microprocessor as a controller derives a control signal from the measurement, and a power amplifier transforms this control signal into a power signal. The control current generates a magnetic field in the electromagnets, so that a magnetic force is produced and the rotor remains in its hovering position. Therefore, essentially the rotor rotates around its geometric axis determined by position sensors. But in practice, the residual unbalance of the rotor makes its inertial axis not coincide with its own geometric axis; when the rotor rotates around its geometric axis, the inertial axis of the rotor will consequently rotate around its own geometric axis, and then the disturbance force and torques are generated by the rotor and transformed to the satellite through its base.

Taking advantage of the ability of the magnetic bearing to actively control the synchronous movement of the rotor can make a high-speed rotor rotate around its inertial axis to reduce the vibration caused by the residual unbalance of rotor.

2.2. Dynamic model of magnetic bearing-rotor system

With respect to MSFW shown in Figure 1, these existing system models of magnetic bearing-rotor with residual unbalance generally regarded the disturbance as an exterior signal of synchronous vibration and inputted it into the displacement signal of the rotor, so that most unbalance vibration control methods try their best to eliminate this disturbance component in the displacement signal of the rotor to avoid generating synchronous motion control currents. But the model of actual magnetic bearing-rotor system P(s) with residual unbalance is shown in Figure 4, where the disturbance d caused by residual unbalance of the rotor is inputted into the magnetic bearing-rotor system as an interior factor of magnetic bearing. The magnetic force F_{AX} is composed of current stiffness component ($K_i i_{AX}$) and displacement stiffness component ($K_h X_A$). Because the rotor displacement caused by the residual unbalance must generate additional disturbing force, even if the synchronous component in the control current has been eliminated, the displacement component of disturbance still exists. This is the real reason why the kinds of control methods that aim to eliminate synchronous component in the current of the magnetic bearing cannot completely eliminate the vibration caused by residual unbalance of rotor.

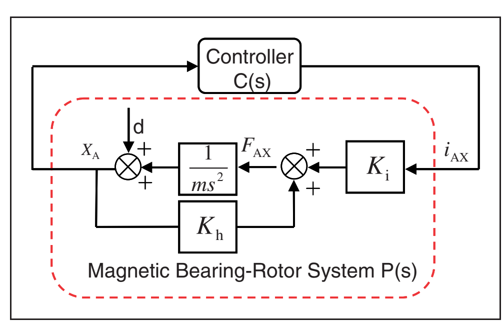

Figure 4. System model of the magnetic bearing-rotor with residual unbalance.

Set N as the origin of the fixed coordinate of Nxy at the central plane of the rotor, and the relationship between the revolving coordinate $o\varepsilon\eta$ and the fixed coordinate Nxy is shown in Figure 5. Set $\vec{l}_0$ as the vectorial displacement from the geometric center O_G to the centroid O_m of rotor, ς the length of $\vec{l}_0$, and θ the angle between O_GO_m and $O_G\varepsilon$. Similarly, as shown in Figure 2, set $\vec{l}_1$ as the vectorial displacement from C_1 to O_1, ξ the length of $\vec{l}_1$, and ϕ the angle between the projectote of $\vec{l}_1$ in the central plane of rotor (Π) and $O_G\varepsilon$. Set $\vec{l}_2$ as the vectorial displacement from C_2 to O_2, ζ the length of $\vec{l}_2$, and φ the angle between the projectote of $\vec{l}_2$ in the central plane of rotor (Π) and $O_G\varepsilon$.

Then the nonlinear magnetic suspension forces of radial magnetic bearing-A and B are expressed as follows:

$$\begin{cases} F_{Ax} = k\left[\left(\dfrac{I_0 + i_{Ax}}{S_0 - X_a\cos\gamma}\right)^2 - \left(\dfrac{I_0 - i_{Ax}}{S_0 + X_a\cos\gamma}\right)^2\right] \\ F_{Ay} = k\left[\left(\dfrac{I_0 + i_{Ay}}{S_0 - Y_a\cos\gamma}\right)^2 - \left(\dfrac{I_0 - i_{Ay}}{S_0 + Y_a\cos\gamma}\right)^2\right] \\ F_{Bx} = k\left[\left(\dfrac{I_0 + i_{Bx}}{S_0 - X_b\cos\gamma}\right)^2 - \left(\dfrac{I_0 - i_{Bx}}{S_0 + Y_b\cos\gamma}\right)^2\right] \\ F_{By} = k\left[\left(\dfrac{I_0 + i_{By}}{S_0 - Y_b\cos\gamma}\right)^2 - \left(\dfrac{I_0 - i_{By}}{S_0 + Y_b\cos\gamma}\right)^2\right] \end{cases} \tag{6}$$

where $k = (N^2 A_s \mu_0 \cos\gamma)/4$, N presents the turns of the coils for the radial magnetic bearing-A or B. A_s presents the working surface of the radial magnetic bearing-A or B (m^2), μ_0 the permeability of free space ($4\pi \times 10^{-7}$H/m). γ the angle between the magnetic pole and y axle (rad). i_{jp} ($j = A, B$; $p = X, Y$) is control current generated by the controller. I_0 the current of the coils for the radial magnetic bearing-A or B when the rotor is in the original position without any drift (A). S_0 is the nominal gap between the stator and rotor of the magnetic bearings (mm). F_{AX}, F_{AY} presents the magnetic suspension force of magnetic bearing-A in direction of X axle or Y axle, respectively. Similarly, F_{BX} F_{BY} presents the magnetic suspension force of magnetic bearing-B in direction of X axle or Y axle, respectively.

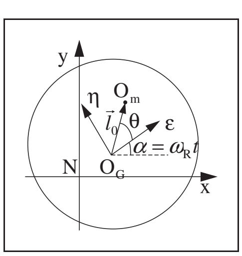

Figure 5. Relationship between coordinate Nxy and coordinate $o\varepsilon\eta$.

If the residual unbalance composed of not only static unbalance but also dynamic unbalance is taken into account, then the displacement relationship between the geometric center and the centroid of the rotor is expressed as

$$\begin{bmatrix} X_A(t) \\ Y_A(t) \\ X_B(t) \\ Y_B(t) \end{bmatrix} = \begin{bmatrix} x_A(t) \\ y_A(t) \\ x_B(t) \\ y_B(t) \end{bmatrix} + \begin{bmatrix} \varsigma\cos(\omega_R t+\theta) - \xi\cos(\omega_R t+\phi) \\ \varsigma\sin(\omega_R t+\theta) + \xi\sin(\omega_R t+\phi) \\ \varsigma\cos(\omega_R t+\theta) + \zeta\cos(\omega_R t+\varphi) \\ \varsigma\sin(\omega_R t+\theta) - \zeta\sin(\omega_R t+\varphi) \end{bmatrix}$$

where X_A, Y_A stands for the displacement of O_1 in the direction of X axle or Y axle in the central plane of magnetic bearing-A, respectively. X_B, Y_B stands for the displacement of O_2 in the direction of X axle or Y axle in the central plane of magnetic bearing-B, respectively. x_A, y_A, x_B, y_B stands for the displacement of centroid of the rotor in the direction of X axle or Y axle in the central plane of magnetic bearing-A or B, respectively.

When the rotor moves within the small neighborhood of its stable point, the nonlinear magnetic suspension forces of radial magnetic bearing-A and B expressed in (6) are linearized as follows,

$$\begin{bmatrix} F_{AX} \\ F_{AY} \\ F_{BX} \\ F_{BY} \end{bmatrix} = K_h \mathbf{E}_{4\times4} \begin{bmatrix} X_A \\ Y_A \\ X_B \\ Y_B \end{bmatrix} + K_i \mathbf{E}_{4\times4} \begin{bmatrix} i_{AX}(X_A) \\ i_{AY}(Y_A) \\ i_{BX}(X_B) \\ i_{BY}(Y_B) \end{bmatrix} \tag{7}$$

Where $K_h = kI_0^2/2S_0^3$ is named as displacement stiffness of magnetic bearing (N/m), $K_i = kI_0/2S_0^2$, named as current stiffness of magnetic bearing (N/m), $\mathbf{E}_{4\times4}$ is an identity matrix.

It can be seen from equation (7) that both the displacement stiffness component and the current stiffness component of the magnetic suspension force contain the signal of unbalance vibration of rotor. According to Newton's second law, the dynamic equation of the magnetic bearing-rotor system with residual unbalance is described as

$$\begin{bmatrix} \ddot{x}_A \\ \ddot{y}_A \\ \ddot{x}_B \\ \ddot{y}_B \end{bmatrix} = \frac{K_h}{m} \mathbf{E}_{4\times4} \begin{bmatrix} X_A \\ Y_A \\ X_B \\ Y_B \end{bmatrix} + \frac{K_i}{m} \mathbf{E}_{4\times4} \begin{bmatrix} i_{AX}(X_A) \\ i_{AY}(Y_A) \\ i_{BX}(X_B) \\ i_{BY}(Y_B) \end{bmatrix} \tag{8}$$

where m stands for the mass of the rotor.

Because these values obtained from position sensors are displacements of the rotor in the central plane of magnetic bearing-A or B, then control currents of the magnetic bearing are obtained based on (8)

$$\begin{bmatrix} i_{AX}(X_A) \\ i_{AY}(Y_A) \\ i_{BX}(X_B) \\ i_{BY}(Y_B) \end{bmatrix} = -\frac{m}{K_i}\mathbf{E}_{4\times4}\left(k_p \begin{bmatrix} X_A \\ Y_A \\ X_B \\ Y_B \end{bmatrix} + k_i \begin{bmatrix} \int X_A \\ \int Y_A \\ \int X_B \\ \int Y_B \end{bmatrix} + k_d \begin{bmatrix} \dot{X}_A \\ \dot{Y}_A \\ \dot{X}_B \\ \dot{Y}_B \end{bmatrix} \right) \tag{9}$$

So the disturbance caused by the residual unbalance of the rotor will affect the displacement signal of rotor. If we denote Θ_{AX}, Θ_{AY}, Θ_{BX} and Θ_{BY} as the individual disturbance in direction of AX, AY, BX and BY, respectively, then

$$\begin{bmatrix} \Theta_{AX}(t) \\ \Theta_{AY}(t) \\ \Theta_{BX}(t) \\ \Theta_{BY}(t) \end{bmatrix} = \varsigma \begin{bmatrix} \cos(\omega_R t + \theta) \\ \sin(\omega_R t + \theta) \\ \cos(\omega_R t + \theta) \\ \sin(\omega_R t + \theta) \end{bmatrix} + \begin{bmatrix} -\xi\cos(\omega_R t + \phi) \\ \xi\sin(\omega_R t + \phi) \\ \zeta\cos(\omega_R t + \varphi) \\ -\zeta\sin(\omega_R t + \varphi) \end{bmatrix} \tag{10}$$

From (9) and (10), we have

$$\begin{bmatrix} X_A(t) \\ Y_A(t) \\ X_B(t) \\ Y_B(t) \end{bmatrix} = \begin{bmatrix} x_A(t) \\ y_A(t) \\ x_B(t) \\ y_B(t) \end{bmatrix} + \begin{bmatrix} \Theta_{AX}(t) \\ \Theta_{AY}(t) \\ \Theta_{BX}(t) \\ \Theta_{BY}(t) \end{bmatrix} \tag{11}$$

Then the dynamic equation group of the magnetic bearing-rotor system with the rotor's static and dynamic unbalance is formed by equations (8), (9), (10) and (11).

3. Compensation method of vibration

3.1. Magnetic suspension force based on synchronous component

From equation (11), (7) can be rewritten as

$$\begin{bmatrix} F_{AX} \\ F_{AY} \\ F_{BX} \\ F_{BY} \end{bmatrix} = K_h\mathbf{E}_{4\times4} \begin{bmatrix} x_A(t) + \Theta_{AX}(t) \\ y_A(t) + \Theta_{AY}(t) \\ x_B(t) + \Theta_{BX}(t) \\ y_B(t) + \Theta_{BY}(t) \end{bmatrix} + K_i\mathbf{E}_{4\times4} \begin{bmatrix} i_{AX}(x_A + \Theta_{AX}) \\ i_{AY}(y_A + \Theta_{AY}) \\ i_{BX}(x_B + \Theta_{BX}) \\ i_{BY}(y_B + \Theta_{BY}) \end{bmatrix} \tag{12}$$

From equation (12), it is clear that the magnetic suspension force consists of a displacement stiffness component and a current stiffness component, but both of these contain synchronous disturbance. Because control current i_{jp} ($j = $ A, B; $p = $ X, Y) is generated by the controller, the goal of most existing unbalance vibration active control methods is to eliminate the synchronous component in control current i_{jp} ($j = $ A, B; $p = $ X, Y) and not to eliminate the synchronous component of the magnetic suspension force. So the synchronous disturbance in the current stiffness component can be eliminated by existing an unbalance vibration active control method, whereas the synchronous component in displacement stiffness must be compensated by a new method to avoid the unbalance force degrading the attitude precision of the satellite platform.

The compensation method of a synchronous component in displacement stiffness proposed by us is to add an additional current, which is equal in magnitude and opposite in direction to the synchronous component, to counteract the synchronous component in the displacement stiffness, i.e., the additional terms of i'_{AX}, i'_{AY}, i'_{BX} and i'_{BY} are added into the control current of magnetic bearing-A and B separately,

$$\begin{bmatrix} i'_{AX} \\ i'_{AY} \\ i'_{BX} \\ i'_{BY} \end{bmatrix} = -\frac{K_h}{K_i}\mathbf{E}_{4\times4} \begin{bmatrix} \Theta_{AX}(t) \\ \Theta_{AY}(t) \\ \Theta_{BX}(t) \\ \Theta_{BY}(t) \end{bmatrix}$$

After the synchronous component in the control current of the magnetic bearing has been eliminated and the synchronous component in the displacement stiffness has been compensated, the magnetic suspension forces are rewritten as

$$\begin{bmatrix} F_{AX} \\ F_{AY} \\ F_{BX} \\ F_{BY} \end{bmatrix} = K_h\mathbf{E}_{4\times4} \begin{bmatrix} x_A \\ y_A \\ x_B \\ y_B \end{bmatrix} + K_i\mathbf{E}_{4\times4} \begin{bmatrix} i_{AX}(x_A) \\ i_{AY}(y_A) \\ i_{BX}(x_B) \\ i_{BY}(y_B) \end{bmatrix} \tag{13}$$

From equation (13), we can see that if all these synchronous components in the magnetic suspension force are eliminated completely, the rotor will rotate around its own inertial axis due to the self-centering ability of the high-speed rotor, and then the vibration caused by the residual unbalance of the rotor is isolated and cannot be transferred to the satellite platform – the stable precision of the satellite can be promoted greatly accordingly.

Because coefficients K_h and K_i are known, then how to identify and determine Θ_{AX}, Θ_{AY}, Θ_{BX} and Θ_{BY} is the key issue to compensate the synchronous component in the magnetic suspension forces.

3.2. Parameter identification of residual unbalance

From equation (10), it is clear that Θ_{AX}, Θ_{AY}, Θ_{BX} and Θ_{BY} are sinusoidal functions with frequency ω_R, so (10) can be rewritten as below, based on the features of synchronous trigonometric function,

$$\begin{bmatrix} \Theta_{AX}(t) \\ \Theta_{AY}(t) \\ \Theta_{BX}(t) \\ \Theta_{BY}(t) \end{bmatrix} = \cos(\omega_R t)\begin{bmatrix} r_{AX1} \\ r_{AY1} \\ r_{BX1} \\ r_{BY1} \end{bmatrix} + \sin(\omega_R t)\begin{bmatrix} r_{AX2} \\ r_{AY2} \\ r_{BX2} \\ r_{BY2} \end{bmatrix} \tag{14}$$

Where $r_{AX1}, r_{AY1}, r_{BX1}, r_{BY1}$ denote these coefficients for the cosine component of synchronous vibration and $r_{AX2}, r_{BX2}, r_{BX2}, r_{BY2}$ denote these coefficients for the sinusoidal component of synchronous vibration, respectively.

From (10) and (14), we can find that there are six parameters in total to depict the static and dynamic unbalance in the dynamic model of the rotor, but for each equation, there are four unbalance parameters, so it is difficult to identify these unbalance disturbance parameters for each magnetic bearing. In (14), the number of parameters to depict the static and dynamic unbalance in the dynamic model of the rotor increases to eight, but for each equation, there are only two unbalance parameters, so the dynamic model of the rotor is simplified and it is easy to identify these unbalance disturbance parameters for each magnetic bearing. As long as the amplitudes of sinusoidal and cosine component of the synchronous vibration in the displacement signal of the rotor are obtained, then Θ_{AX}, Θ_{AY}, Θ_{BX} and Θ_{BY} are determined accordingly.

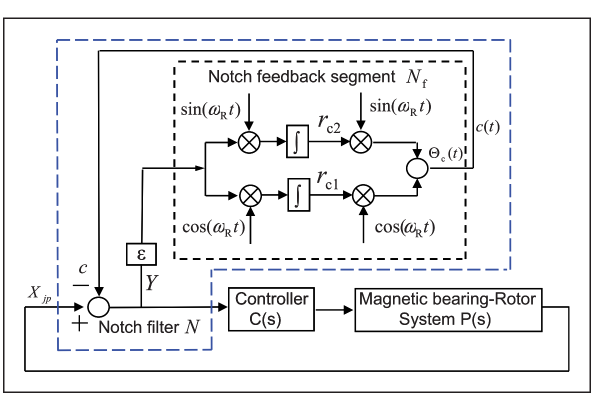

Figure 6. Principle of adaptive notch filter.

As the paper presented by Liu et al. (2010), $\Theta_{jp}(t)$ $(j = \mathrm{A,B}; p = \mathrm{X,Y})$ can be identified by adaptive notch filter whose center notching frequency varies with the speed of the rotor because the synchronous disturbance of $\Theta_{jp}(t)\,(j = \mathrm{A,B}; p = \mathrm{X,Y})$ is a sinusoidal function with frequency ω_R in the displacement signal of rotor. As an example, the work principle of the notch filter for the identification of Θ_{AX} is shown in Figure 6, the key segment of notch filter N is the notch feedback N_f, whose center notching frequency varies with the speed of the rotor, both the convergent speed and the bandwidth of the center notch are determined by ε.

Set $\omega(t)$ and $c(t)$ as the inputting and outputting of notch feedback segment N_f, respectively, then

$$c(t) = \begin{bmatrix} \sin(\omega_R t) & \cos(\omega_R t) \end{bmatrix} \cdot \begin{bmatrix} \int \sin(\omega_R t)\cdot\omega(t)\mathrm{d}t \\ \int \cos(\omega_R t)\cdot\omega(t)\mathrm{d}t \end{bmatrix}$$

Where c and ω satisfy the equation $\ddot{c} + \omega_R^2 c = \dot{\omega}$

Then the transfer function of N_f is

$$N_f(s) = c(s)/\omega(s) = s/(s^2 + \omega_R^2) \tag{15}$$

From (15), it is clear that when $X_{jp}(t)\,(j = \mathrm{A,B}; p = \mathrm{X,Y})$ is the inputting and $c(t)$ is the outputting of notch filter N, the transfer function T(s) of notch filter is T$(s) = c(s)/X_{jp}(s) = \varepsilon s/(s^2 + \varepsilon s + \omega_R^2)$.

Let $s = \mathrm{j}\omega$, when $\varepsilon \neq 0$, we have

$$\begin{cases} N_o(\mathrm{j}\omega) \approx 0.[\omega \in (0, \omega_R - \Delta\omega) \cup (\omega_R + \Delta\omega, \infty)] \\ N_o(\mathrm{j}\omega) = 1.[\omega \in (\omega_R - \Delta\omega, \omega_R + \Delta\omega)] \end{cases} \tag{16}$$

Equation (16) implies that when $\varepsilon \neq 0$, the outputting of notch filter N is approximate to the component with frequency ω_R in the inputting $X_{jp}(t)$ $(j = \mathrm{A,B}; p = \mathrm{X,Y})$. From Figure 6, it is clear that the outputting $c(t)$ of notch filter N is the outputting $\Theta_c(t)$ of notch feedback segment N_f. From (10) and (11), the component with frequency ω_R in the inputting of notch filter N is $\Theta_{jp}(t)\,(j = \mathrm{A,B}; p = \mathrm{X,Y})$, i.e., when $t \to \infty$, $\Theta_c(t) \to \Theta_{jp}(t)(j = \mathrm{A,B}; p = \mathrm{X,Y})$

From Figure 6, the outputting $\Theta_c(t)$ of notch feedback segment N_f is

$$\Theta_c(t) = r_{c1}\cos(\omega_R t) + r_{c2}\sin(\omega_R t) \tag{17}$$

Comparing (17) with (14), we obtained

$$\begin{cases} r_{AX1} = r_{c1} \\ r_{AX2} = r_{c2} \end{cases}$$

This means when the feedback segment converges, the amplitude of the outputting of integrator in the notch feedback segment is equal to that of the sinusoidal and cosine component in synchronous vibration contained in the displacement signal of rotor, then the identification of unbalance vibration parameters in the rotor's displacement signal is realized.

3.3. Method of magnetic suspension force compensation

Based on the notch filter, a magnetic suspension force compensation method proposed by us is to take the displacement stiffness component in the disturbance force caused by residual unbalance of the rotor as feed-forward and imposed it into the magnetic bearing-rotor system. The diagram of the magnetic suspension force compensation method is shown in Figure 7(a), Figure 7(b) is its equivalent diagram.

The transfer function of the modified notch filter is

$$\mathrm{N}(s) = Y(s)/X_{\mathrm{A}}(s) = (s^2 + \omega_{\mathrm{R}}^2)/(s^2 + \omega_{\mathrm{R}}^2 + \varepsilon s) \tag{18}$$

From Figure 7(b), the transfer function of the magnetic bearing-rotor system is

$$\mathrm{P(s)} = \mathrm{K_i}/(\mathrm{m}s^2 - \mathrm{K_h}) \tag{19}$$

The controller C is the classic proportional-integral-derivative (PID)-controller, its transfer function is

$$\mathrm{C(s)} = -(\mathrm{k_p} + \mathrm{k_d}s + \mathrm{k_i}/s) \tag{20}$$

Where $\mathrm{k_p}$ is proportionality coefficient, $\mathrm{k_i}$ integration coefficient, and $\mathrm{k_d}$ differential coefficient.

Then the closed-loop eigen equation of the magnetic bearing -rotor system is

$$1 + \mathrm{N}(s)\left(\mathrm{C}(s) - \frac{\varepsilon \mathrm{K_h}}{\mathrm{K_i}} \cdot N_{\mathrm{f}}(s)\right) \cdot \mathrm{P}(s) = 0 \tag{21}$$

Because the feedback segment of the closed-loop system for the magnetic bearing-rotor system is modified by the feed-forward of displacement stiffness component to compensate the disturbance force, it is necessary to analyze the stability of the magnetic bearing-rotor system.

4. Stability analysis of the unbalance vibration active control method

4.1. Stability of rotor in beyond critical stable speed

The stability analysis method of the magnetic bearing-rotor system with magnetic suspension force compensation is root locus. The precondition of stability analysis is that the closed-loop control system for its original magnetic bearing-rotor system is stable, i.e., the eigen equation of the origin closed-loop system $1 + \mathrm{P}(s) \cdot \mathrm{C}(s) = 0$ has negative real part, then

$$\mathrm{m}s^3 + \mathrm{K_i k_d}s^2 + (\mathrm{K_i k_p} - \mathrm{K_h})s + \mathrm{K_i k_i} = 0 \tag{22}$$

With respect to equation (20), according to the algebraic criterion of the eigen root, we obtain

$$\begin{cases} \mathrm{k_p} > \mathrm{K_h}/\mathrm{K_i} \\ \mathrm{k_i}/\mathrm{k_d} < (\mathrm{K_i k_p} - \mathrm{K_h})/\mathrm{m} \\ \mathrm{k_i} > 0 \end{cases} \tag{23}$$

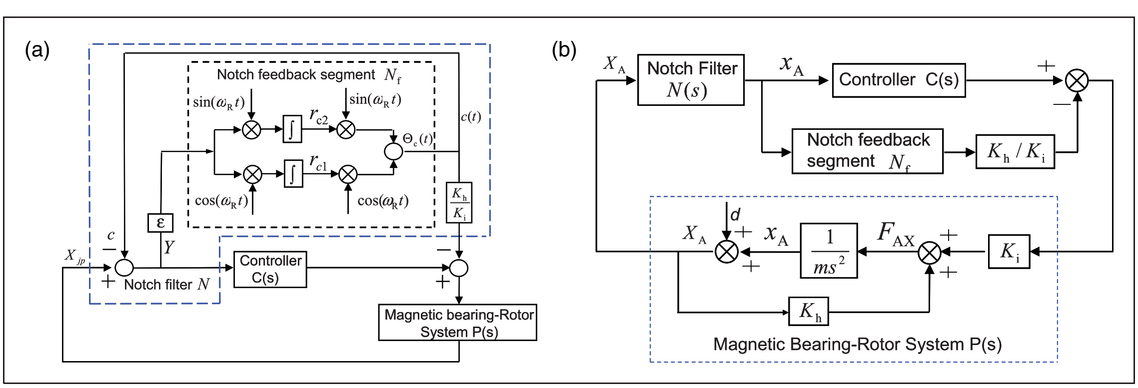

Figure 7. Diagram of magnetic suspension force compensation and its equivalent. (a) Diagram of magnetic suspension force compensation; (b) Equivalent diagram of magnetic suspension force compensation.

Substitute (15), (18), (19) and (20) into (21), we obtain

$$1+\frac{[\mathrm{m}s^3+\mathrm{K_ik_d}s^2+(\mathrm{K_ik_p}-\mathrm{K_h})s+\mathrm{K_ik_i}]\omega_\mathrm{R}^2}{\mathrm{m}s^5+(\varepsilon\mathrm{m}+\mathrm{K_ik_d})s^4+(\mathrm{K_ik_p}-\mathrm{K_h})s^3+(\mathrm{K_ik_i}-2\varepsilon\mathrm{K_h})s^2} =0 \tag{24}$$

Therefore, (24) and (21) have the same eigen roots; we can obtain the distribution feature of (24) by analysis that of (21).

Taking ω_R^2 as the variant, the distribution of the eigen root for (24) can be determined by analyzing the distribution of eigen root for its corresponding open-loop system. From (24), there are five poles and three zeroes. When ω_R^2 changes from 0 to ∞, there are five embranchments totally, and the embranchment of the root locus begins from the pole point of the open-loop system and terminates at the zero point of its open-loop system. The distribution of poles and zeros for the open-loop system are analyzed as follows.

From (24), the poles of the open-loop system are given by

$$\mathrm{m}s^5+(\varepsilon\mathrm{m}+\mathrm{K_ik_d})s^4+(\mathrm{K_ik_p}-\mathrm{K_h})s^3 + (\mathrm{K_ik_i}-2\varepsilon\mathrm{K_h})s^2=0 \tag{25}$$

Based on the algebraic criterion of stability, the case of stability is

$$\begin{cases} \mathrm{k_p}>\mathrm{K_h}/\mathrm{K_i} \\ [\mathrm{K_ik_d}(\mathrm{K_ik_p}-\mathrm{K_h})-\mathrm{mK_ik_i}]+\varepsilon\mathrm{m}(\mathrm{K_ik_p}+\mathrm{K_h})>0 \\ \mathrm{k_i}>2\varepsilon\ \mathrm{K_h}/\mathrm{K_i} \end{cases} \tag{26}$$

From equation (23), it is clear that the former two cases come into existence, but the third case cannot be derived from the stability of the original system. Accordingly, there maybe exist positive root for those poles of its open-loop system, i.e., the eigen root maybe start from the positive half s-plane when ω_R^2 changes.

From (24) and (22), we can see that zeros of the open-loop system are the poles of the closed-loop system, i.e., the poles root locus of the closed-loop system for the magnetic suspension force compensation tends to the poles of its origin closed-loop system. From the precondition of the stability for the original closed-loop system, all poles and zeros are distributed in the left s-plane. Because there are five embranchments of the root locus arising from the poles of the open-loop system, but there are only three zeros for the open-loop system, it is necessary to discuss the distribution of the other two embranchments of the root locus. According to the classic control theorem, there are two embranchments of the root locus tending to the infinite distance along its asymptote. Set the skew angle of the asymptote with real axis of s plane as ϕ_a, the cross point with real axis of s plane as σ_a, then ϕ_a and σ_a of the asymptote with real axis of s plane are analyzed as follows.

Modify the eigen equation of the closed-loop system as

$$\frac{[\mathrm{m}s^3+\mathrm{K_ik_d}s^2+(\mathrm{K_ik_p}-\mathrm{K_h})s+\mathrm{K_ik_i}]\omega_\mathrm{R}^2}{\mathrm{m}s^5+(\varepsilon\mathrm{m}+\mathrm{K_ik_d})s^4+(\mathrm{K_ik_p}-\mathrm{K_h})s^3+(\mathrm{K_ik_i}-2\varepsilon\ \mathrm{K_h})s^2} =-1 \tag{27}$$

When $\omega_\mathrm{R}^2\to\infty$, $s\to\infty$, then (27) is expressed approximately as

$$s^2(1+\varepsilon/s)=-\omega_\mathrm{R}^2 \text{ or } s\sqrt{(1+\varepsilon/s)}=\sqrt{-\omega_\mathrm{R}^2} \tag{28}$$

Extend the left side of (28) according to the Newton binominal formula and linearize it, we have $s(1+\varepsilon/2s)=\sqrt{-\omega_\mathrm{R}^2}$.

That is

$$s+\varepsilon/2=\sqrt{-\omega_\mathrm{R}^2} \tag{29}$$

Substitute $-1=\mathrm{e}^{\mathrm{j}(2\mathrm{k}+1)\pi}$, $(\mathrm{k}=0,1,2,\ldots)$ into (29), then

$$s=-\varepsilon/2+\omega_\mathrm{R}\cdot\mathrm{e}^{\mathrm{j}\pi(2\mathrm{k}+1)/2},\ (\mathrm{k}=0,1,2,\ldots) \tag{30}$$

Equation (30) is the equation of the asymptote when $\omega_\mathrm{R}^2\to\infty$, and

$$\begin{cases} \sigma_\mathrm{a}=-\varepsilon/2 \\ \phi_\mathrm{a}=(2\mathrm{k}+1)\pi/2, (\mathrm{k}=0,1) \end{cases}$$

In short, there are five embranchments totally for the closed-loop eigen equation, even though there is a certain initial point starting from the right-half s-plane when $\omega_\mathrm{R}^2=0$, but when $\omega_\mathrm{R}^2\to\infty$, there are three embranchments tending to their three eigen roots of the original stable closed-loop system, the left two embranchments tend to their asymptote in the left s-plane. Because of the continuity of the root locus, the magnetic suspension force compensation method is stable where ω_R^2 is large enough.

If we defined the speed at which the embranchments of the root locus across the imaginary axis as the critical stable speed of rotor, it is obvious that the magnetic suspension force compensation method is stable when the speed of the rotor is beyond its critical stable speed.

4.2. Critical stable speed of rotor

Because the critical stable speed of the rotor is very important for the magnetic suspension force compensation method, we need to discuss the critical stable speed of the rotor and analyze the cross point value of the root locus and the imaginary axis.

Set the cross point of the root locus and the imaginary axis as $s = j\omega$, which satisfies the eigen equation of the closed-loop, i.e., substitute $s = j\omega$ into the eigen equation of the closed-loop, both the real part and imaginary part are zero.

$$\begin{cases} \omega \cdot (\omega^2 \mathrm{m} + \mathrm{K_h} - \mathrm{K_i k_p}) \cdot (\omega_\mathrm{R}^2 - \omega^2) = 0 \\ (\mathrm{K_i k_d}\omega^2 - \mathrm{K_i k_i})(\omega_\mathrm{R}^2 - \omega^2) - (\omega^4 \varepsilon \mathrm{m} + 2\varepsilon\omega^2 \mathrm{K_h}) = 0 \end{cases} \tag{31}$$

From the first sub-equation in (31), there are three possibilities to chose ω (taking the cross points in the upper s-plane into account only, the cross points in the lower s-plane can be obtained due to the symmetry of s plane)

$$\begin{cases} \omega = 0 \\ \omega = \sqrt{(\mathrm{K_i k_p} - \mathrm{K_h})/\mathrm{m}} \\ \omega = \omega_\mathrm{R} \end{cases} \tag{32}$$

In equation (31), a second sub-equation exists only when $\omega = \sqrt{(\mathrm{K_i k_p} - \mathrm{K_h})/\mathrm{m}}$ or $\omega = \omega_\mathrm{R} = 0$.

For (24), if $\omega = \omega_\mathrm{R} = 0$, the embranchments of the root locus will start from the origin of the coordinate, which isn't the critical stable speed or the crossing point discussed. Therefore, the cross point for the root locus and the imaginary axis is

$$\omega = \sqrt{(\mathrm{K_i k_p} - \mathrm{K_h})/m} \tag{33}$$

Substituting (33) into second sub-equation in (31), the critical stable speed $\omega_{\mathrm{R-critical}}$ of the rotor is obtained

$$\omega_{\mathrm{R-critical}} = \pm\sqrt{\frac{\mathrm{K_i}(\mathrm{K_i k_p} - \mathrm{K_h})[(\mathrm{K_i k_p} - \mathrm{K_h}) \cdot \mathrm{k_d} - \mathrm{k_i m}] + \varepsilon \mathrm{m}(\mathrm{K_i^2 k_p^2} - \mathrm{K_h^2})}{\mathrm{K_i m}[(\mathrm{K_i k_p} - \mathrm{K_h}) \cdot \mathrm{k_d} - \mathrm{k_i m}]}} \tag{34}$$

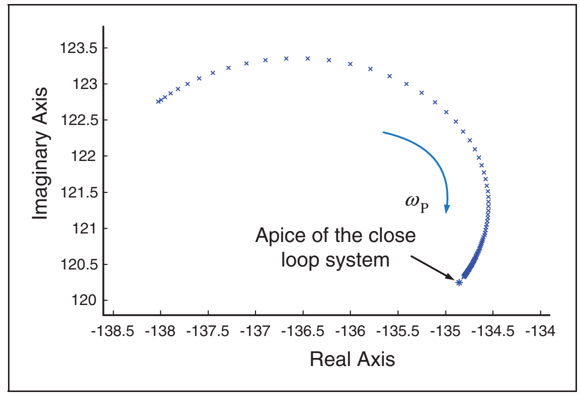

Figure 8. Embranchment of root locus tends to the origin of the coordinate in pole-zero map.

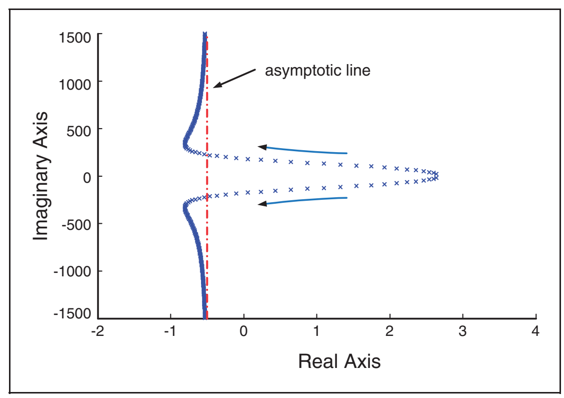

Figure 9. Embranchment of root locus tends to their asymptote in pole-zero map.

From (34), when ε is fairly small, (34) can be simplified as

$$\omega_{\mathrm{R-critical}} \approx \pm\sqrt{(\mathrm{K_i k_p} - \mathrm{K_h})/\mathrm{m}} \tag{35}$$

Which means the critical stable speed of rotor $\omega_{\mathrm{R-critical}}$ is equal to the cross point of the root locus and the imaginary axis approximately.

When ω_R changes from zero to infinity, the embranchments' distribution of root locus for the closed-loop magnetic suspension force compensation are shown in Figure 8 and Figure 9.

Figure 8 displays these embranchments tending to the origin of the coordinate. Because these three embranchments tend to the eigen root of the closed-loop system infinitely, they must be located in the left-half s-plane ultimately. Figure 9 displays embranchment tending to their asymptote. Even if the start points of these root locuses locate in the right-half s-plane, they tend to their asymptote in the left-half s-plane ultimately.

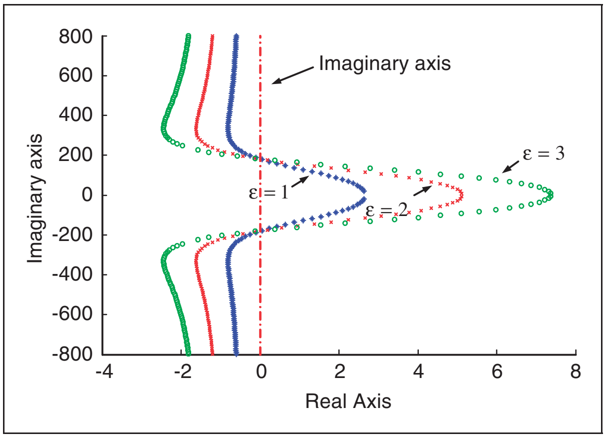

Figure 10. Effect of ε on the embranchment of root locus in pole-zero map.

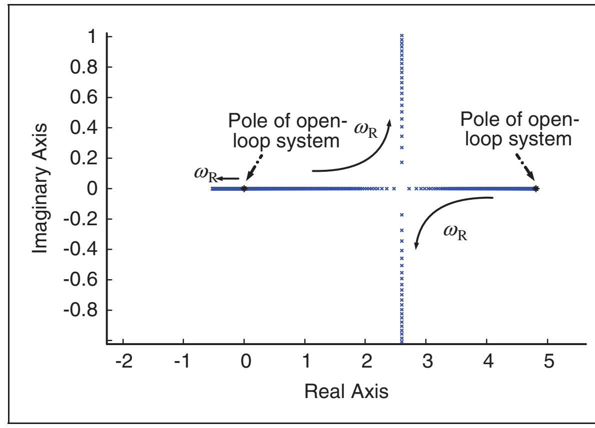

Figure 12. Root locus of the open-loop control system with one right root.

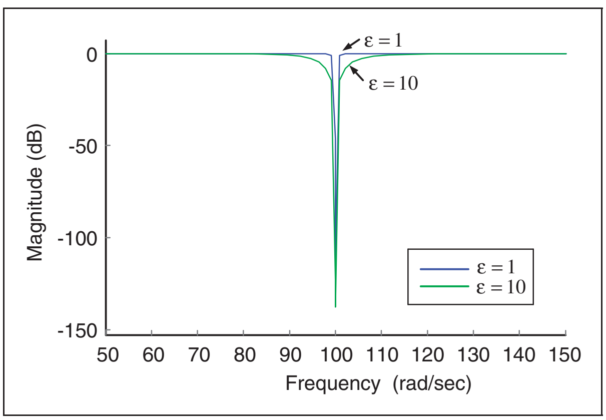

Figure 11. Effect of ε on the frequency of control system.

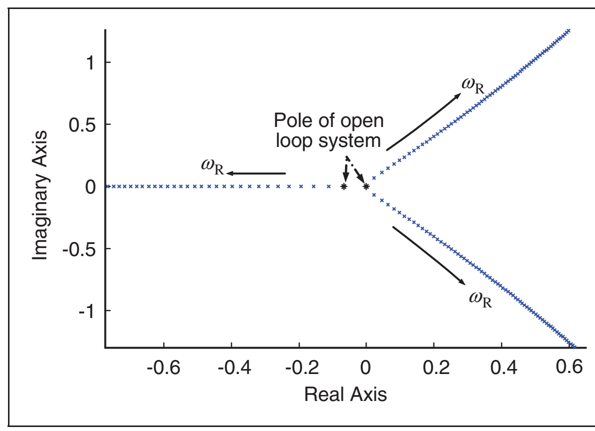

Figure 13. Root locus of the open-loop control system without right roots.

Figure 10 illustrate the effect of ε on the embranchment of the root locus, ε determines the asymptote and starting point of the root locus, but neither affects the critical stable speed of rotor nor do they affect the crossing point in the imaginary axis. Because the cross point of the asymptote and real axis is $-\varepsilon/2$, then the distance between the poles of the closed-loop system and the real axis is determined by ε, i.e., the convergent speed of algorithm for the magnetic suspension force compensation method is determined by ε. The larger that ε was, the more rapid the convergent speed of algorithm is. On the other hand, ε determines the bandwidth of the notch filter as shown in Figure 11. With increasing ε, the filtering effect of the notch filter becomes worse, i.e., the identification precision of the unbalance vibration is determined by ε, and the identification precision of the unbalance parameters for the proposed vibration suppression method becomes worse with ε increasing. In practice, ε is often as little as possible to obtain an ideal level of identification precision of the unbalance vibration in case the arithmetic of the vibration suppression method can trace the speed of rotor stably.

From equation (33), it is known that there are two crossing points of the pole root locus of the closed-loop system and the imaginary axis, i.e., $\pm\sqrt{(K_i k_p - K_h)/m}$. But according to the algebraic stable criterion, there is at most one root locating in the right-half plane, so it is necessary to analyze the relationship between the number of right roots and the crossing points of embranchments of the root locus and the imaginary axis.

For equation (23), the root locus is shown in Figure 12 when $0 < k_i < 2\varepsilon\, K_h/K_i$. There is one root locating in the right-half plane. Among these two embranchments, one turns left and tends to the zero of the open-loop system, another turns right, intersects with

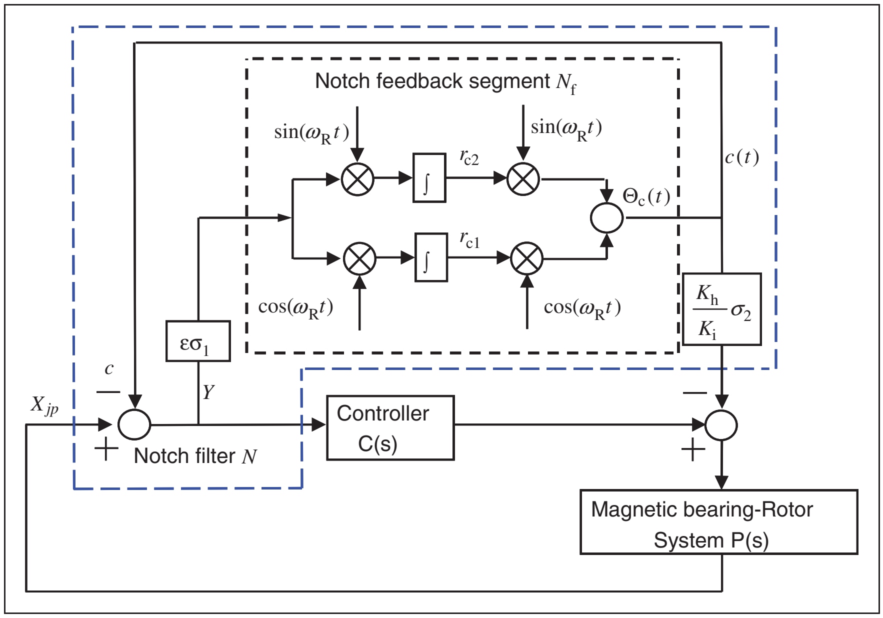

Figure 14. Open-loop type of magnetic suspension force compensation.

the embranchments starting from the right root of the open-loop system before departing from the real axis, and finally intersects with the imaginary axis. When $k_i > 2\varepsilon K_h/K_i$, the root locus is shown in Figure 13. All poles of the open-loop system locate in the left-half s-plane, two embranchments locating at the origin of the coordinate enter the right-half s-plane and finally intersect with the imaginary axis.

4.3. Stability of rotor under critical stable speed

The speed range of the rotor is within 600 rpm and 5000 rpm (10–83 Hz) in practice, but the proposed vibration suppression method has positive root over $(-\sqrt{(K_i k_p - K_h)/m}, \sqrt{(K_i k_p - K_h)/m})$, which is also shown in Figure 8. On the other hand, equation (35) has implied that the critical stable speed $\omega_{R-\text{critical}}$ of the rotor is determined by characteristics of the magnetic bearing such as K_i, K_h, k_p, m and so on, and with respect to the MSFW shown in Figure 1, $\omega_{R-\text{critical}} \approx 50$ Hz. So there exists the unstable problem of the rotor, in that the speed of the rotor repeatedly traverses the critical stable speed.

Because the unbalance of the rotor is a deterministic physical property and does not change with the its speed, so the unbalance parameters of the rotor identified by previous methods where the speed of the rotor is beyond its critical stable speed are reusable. When the speed of the rotor is less than the critical stable speed, the open-loop type of magnetic suspension force compensation shown in Figure 14 can suppress the vibration caused by the residual unbalance of the rotor.

As shown in Figure 14, two switchers $\sigma_1, \sigma_2 \in \{0, 1\}$ are added to the previous introduced vibration suppression method to form the modified vibration suppression method, which is fit to suppress the vibration of the rotor in the whole speed range. σ_1 is the switcher to turn on or turn off the magnetic suspension force compensation system. When the adaptive notch filter N converges, the inputting of the adaptive notch filter N is turned off by σ_1, then the synchronous vibration in the displacement signal is compensated by the open-loop method based on the unbalance parameters identified previously. σ_2 is the switcher to turn on or turn off the compensation operation of the displacement stiffness component in the magnetic bearing force.

Steps of the open-loop magnetic suspension force compensation are:

(i) At initial state $(\sigma_1, \sigma_2) = (0, 0)$, both the adaptive notch filter N and the compensation of the displacement stiffness component do not work, and the rotor rotates around its own geometric axis
(ii) When the speed of the rotor is beyond its own critical stable speed, let $(\sigma_1, \sigma_2) = (1, 0)$, the synchronous component with frequency ω_R in the signal of the rotor's displacement are eliminated, so the unbalance component in the rotor's displacement is identified while the synchronous component in the controlling current is eliminated. Thus the synchronous movement in the current

stiffness component is absent, but the synchronous movement in the displacement stiffness component still exists

(iii) After the synchronous movement in the displacement signal is eliminated by notch filter N completely, let $(\sigma_1, \sigma_2) = (1,\ 1)$, and eliminate the synchronous movement in the displacement stiffness component by the magnetic suspension force compensation method. Now the constraints of magnetic bearings on the synchronous movement are eliminated completely, the rotor rotates around its own inertial axis, the vibration caused by unbalance of the rotor is isolated, and

(iv) After the rotor rotates around its own inertial axis, let $(\sigma_1, \sigma_2) = (0,\ 1)$, turn off the inputting of notch filter N, and compensate the current stiffness component and displacement stiffness component in the magnetic suspension force based on these identified unbalance parameters and the angular position of the rotor generated from the optic-electric encoder or the array of hall sensors.

4.4. *Compensation of magnetic bearing force for N octave vibration*

When the unbalance vibration is n octave (n = 1, 2, 3...) the transfer function of the notch filter becomes $N'(s)$, and $N'(s) = \left[s^2 + (n\omega_R)^2\right] / \left[s^2 + (n\omega_R)^2 + \varepsilon s\right]$

The transfer function of the notch feedback segment becomes $N'_f(s) = c(s)/\omega(s) = s/[s^2 + (n\omega_R)^2]$

The eigen equation of the system becomes

$$\frac{[ms^3 + K_i k_d s^2 + (K_i k_p - K_h)s + K_i k_i](n\omega_R)^2}{ms^5 + (\varepsilon m + K_i k_d)s^4 + (K_i k_p - K_h)s^3 + (K_i k_i - 2\varepsilon\, K_h)s^2} = -1 \tag{36}$$

From (36) and (27), it is clear that the distribution of poles and zeros for n octave is the same as that of the synchronous vibration suppression system.

Set the cross point of the root locus and the imaginary axis as $s = j\omega$, then the critical stable speed and cross point of the root locus and the imaginary axis are obtained.

$$\begin{cases} \omega \cdot (\omega^2 m + K_h - K_i k_p) \cdot [(n\omega_R)^2 - \omega^2] = 0 \\ (K_i k_d \omega^2 - K_i k_i)[(n\omega_R)^2 - \omega^2] - (\omega^4 \varepsilon m + 2\varepsilon\omega^2 K_h) = 0 \end{cases} \tag{37}$$

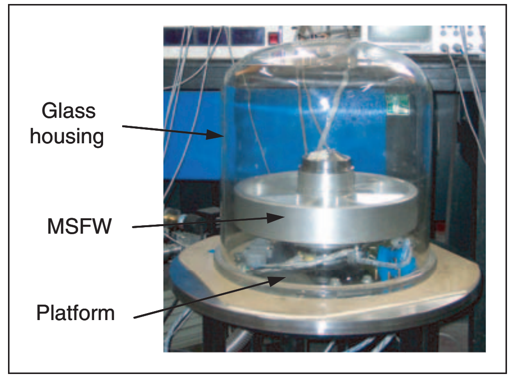

Figure 15. Magnetically suspended flywheel (MSFW) with angular momentum 50 Nms.

The traversing point is $\omega = \sqrt{(K_i k_p - K_h)/m}$. The related critical stable speed $\omega'_{R-\text{critical}}$ is

$$\omega'_{R-\text{critical}} = \pm\frac{1}{n}\sqrt{\frac{K_i(K_i k_p - K_h)[(K_i k_p - K_h)\cdot k_d - k_i m] + \varepsilon m(K_i^2 k_p^2 - K_h^2)}{K_i m[(K_i k_p - K_h)\cdot k_d - k_i m]}} \tag{38}$$

When ε is fairly small, (39) can be simplified as

$$\Omega' = \pm\frac{1}{n}\sqrt{\frac{K_i k_p - K_h}{m}} \tag{39}$$

That is to say when the frequency of vibration is n times that of the synchronous vibration, the critical stable speed is 1/n times that of the suppression of the synchronous vibration.

5. Experimental research

The experimental research done with MSFW is shown in Figure 15 to verify the validity of this vibration suppression method, and the main parameters of MSFW with angular momentum 50 Nms are listed in Table 1. The MSFW is equipped with an optic-electric encoder to detect the relative and absolute angular position of the rotor, the digital controller is mainly made up of TMS320C6713B + FPGA. The glass housing is used to keep the pressure in the enclosure at about 1 ~ 2 Pa.

In order to detect the vibration of the flywheel caused by the residual unbalance of its rotor, the vibration testing platform made up of acceleration sensors, as shown in Figure 16, has been produced. The bracket is used to mount the flywheel, the acceleration sensors with sensitivity of about 1500 mV/g are distributed on the bracket and used to measure the vibration. On the crisscross bracket, there is one acceleration sensor, which is used to measure the vibration in the Z

Table 1. Parameters of 5-degrees-of-freedom magnetically suspended flywheel

Symbol	Parameter	Designed values
Ω	Nominal speed of rotor	5000 rpm
m	Mass of rotor	7.35 Kg
Φ	Maximal diameter of rotor	340 mm
K_i	Current stiffness of magnetic bearings	300 (N/A)
K_h	Displacement stiffness of magnetic bearings	6.68×10^5 N/m
k_s	Sensitivity of position sensor	0.075 V/μm
k_p	Proportional coefficient of the control circuit	6.03
k_d	Differential coefficient of the control circuit	0.006621
k_i	Integral coefficient of the control circuit	0.4285

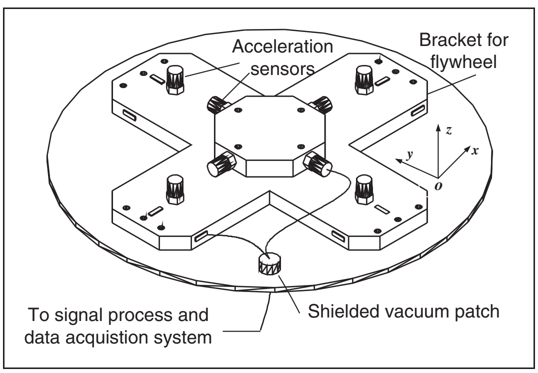

Figure 16. Vibration test platform for magnetically suspended flywheel.

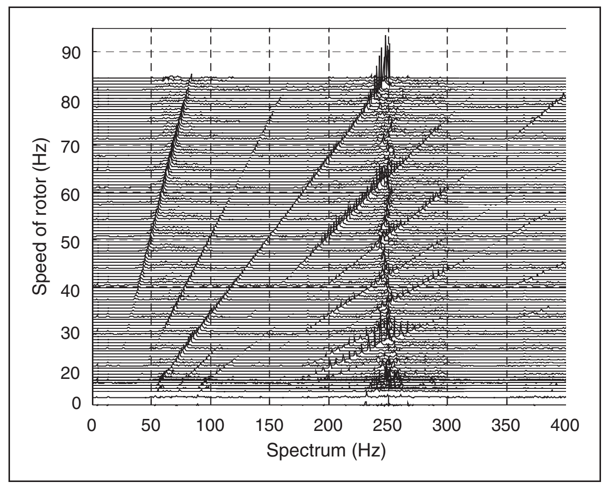

Figure 18. Slow-down waterfall of magnetically suspended flywheel with vibration suppression.

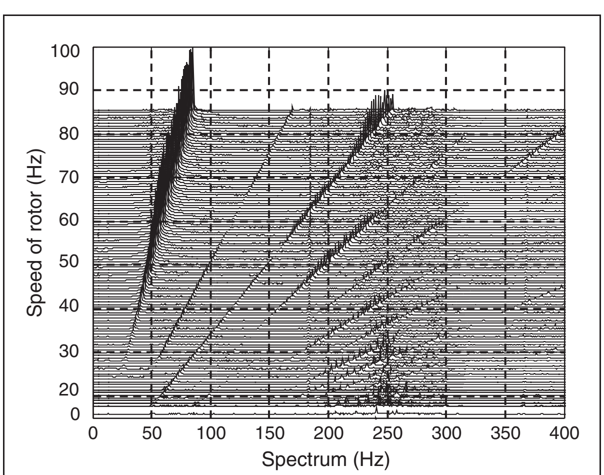

Figure 17. Slow-down waterfall of magnetically suspended flywheel without vibration suppression,.

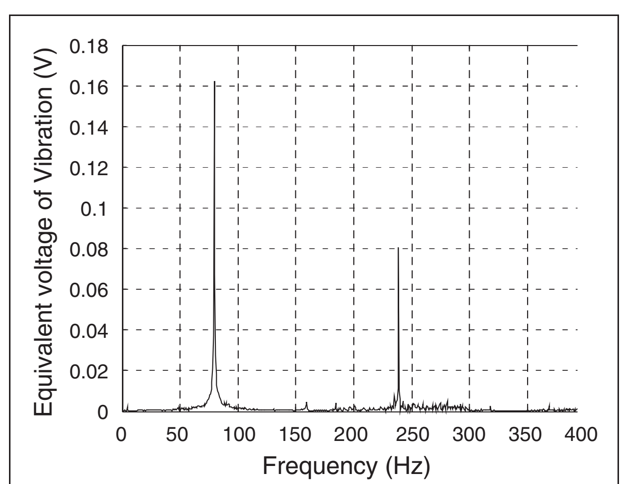

Figure 19. Amplitude of vibration of rotor (at 80 Hz) without vibration suppression.

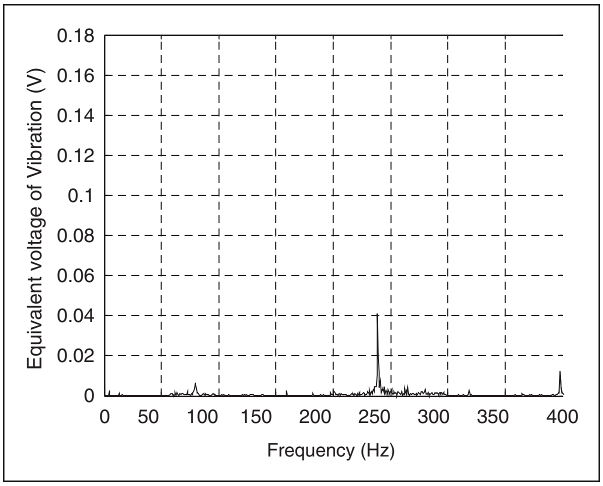

Figure 20. Amplitude of vibration of rotor (at 80 Hz) with vibration suppression.

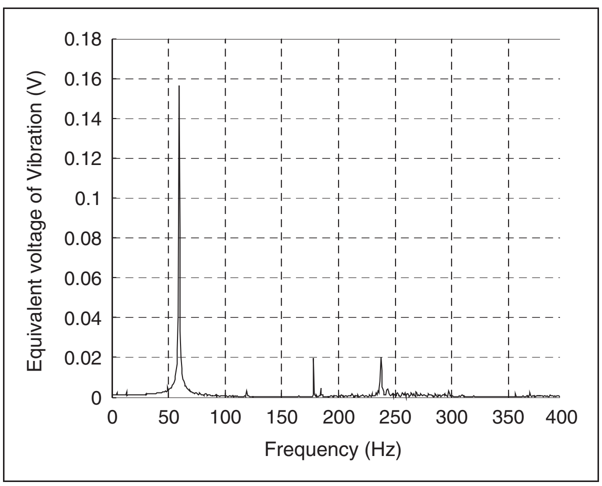

Figure 21. Amplitude of vibration of rotor (at 60 Hz) without vibration suppression.

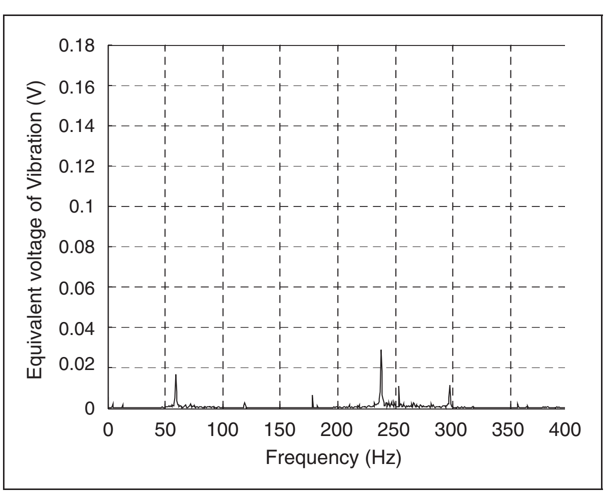

Figure 22. Amplitude of vibration of rotor (at 60 Hz) with vibration suppression.

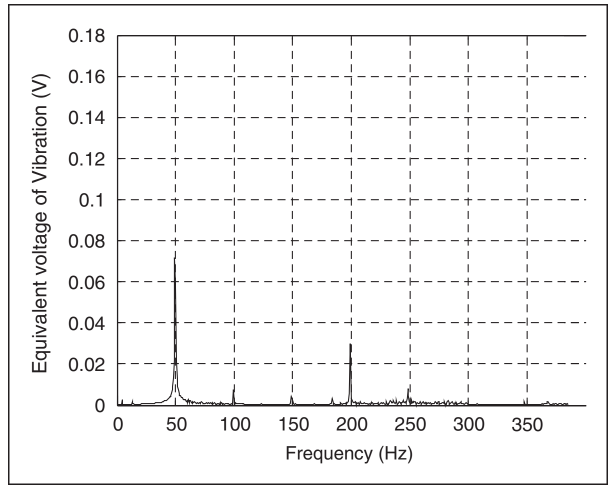

Figure 23. Amplitude of vibration of rotor (at 50 Hz) without vibration suppression.

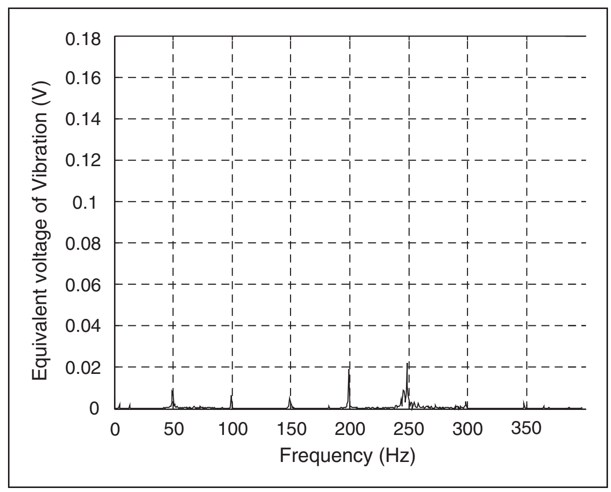

Figure 24. Amplitude of vibration of rotor (at 50 Hz) with vibration suppression.

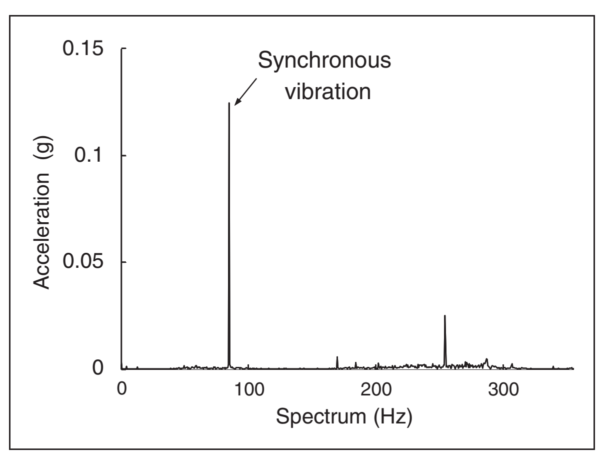

Figure 25. Spectrum of rotor vibration without vibration suppression.

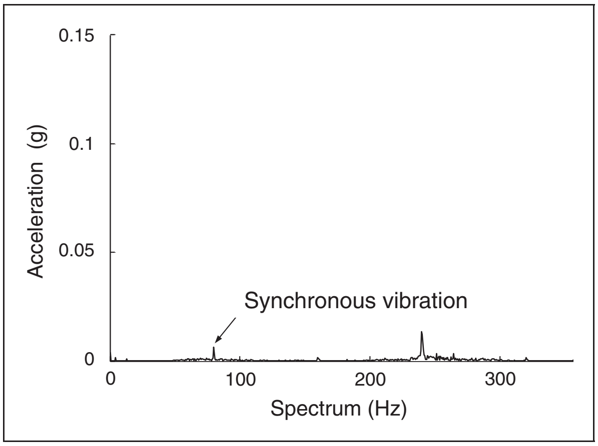

Figure 26. Spectrum of rotor vibration with vibration suppression.

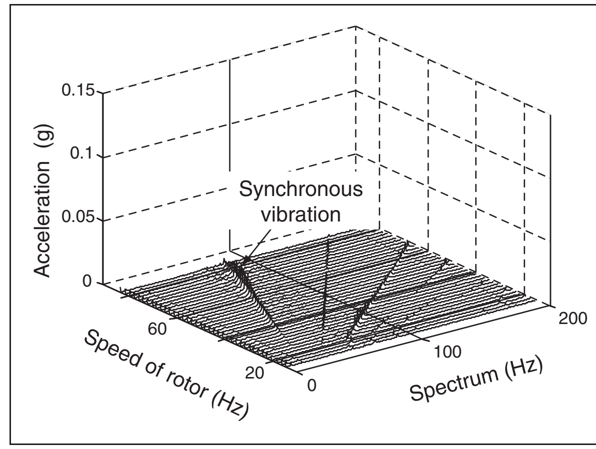

Figure 28. Waterfall of rotor vibration with vibration suppression.

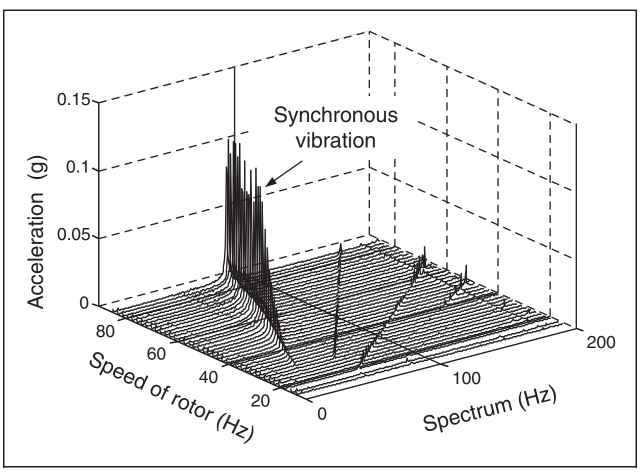

Figure 27. Waterfall of rotor vibration without vibration suppression.

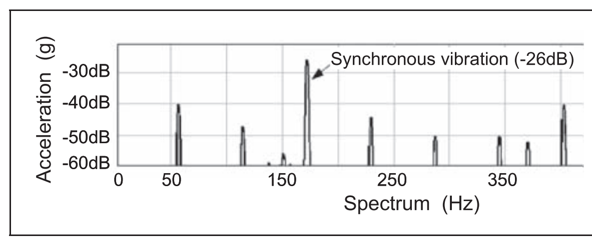

Figure 29. Vibration spectrum of high precision balanced rotor.

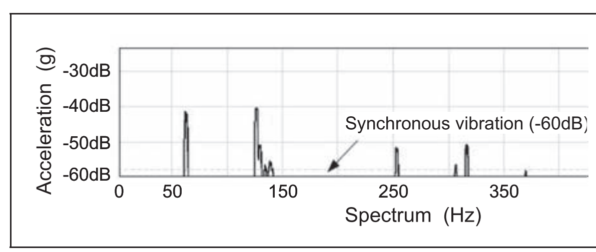

Figure 30. Vibration spectrum of high precision balanced rotor with vibration suppression.

direction of the flywheel and is fixed in the direction of X+, X−, Y+ and Y−, respectively. On the octagon bracket, there is one acceleration sensor fixed in the direction of X+ or X- respectively to measure the vibration in the direction X. Similarly, there is one acceleration sensor fixed in the direction of Y+ or Y- respectively to measure the vibration in the direction Y.

The vibration testing method is to enclose the MSFW in a vacuum housing with pressure about $1 \sim 2$ Pa, then speed up the rotor by the embedded motor. When the speed is up to 5000 rpm, turn off the power of the motor, so the rotor will slow down freely in the vacuum housing. During the slowing down process, the main components and their amplitudes of the radial vibration for MSFW are measured within the whole speed range. Figure 17 illustrates the radial vibration of MSFW without any vibration suppression method, and Figure 18 illustrates the radial vibration of MSFW with the proposed vibration suppression method, respectively. It is clear that the synchronous component in the vibration caused by the residual unbalance of the rotor have been eliminated greatly.

Because the vibration of the rotor is measured by position sensors and their outputting are voltages, so the vibration value of the rotor is equal to the voltage multiplied by the sensitivity of position sensor listed in Table 1. Figures 19 and 20, Figures 21 and 22, and Figures 23 and 24 illustrate the measured vibration amplitude of the rotor without or with vibration suppression method at speed of 4800 rpm (80 Hz), 3600 rpm (60 Hz), or 2500 rpm (50 Hz), respectively.

When the speed of the rotor is beyond its critical stable speed (as for MSFW shown in Figures 1 and 15, the critical stable speed is about 3000rpm (50HZ)), the elimination effect of the synchronous component in the magnetic suspension force is measured. Figure 25 illustrates the spectrum of vibration of the rotor without vibration suppression. Without any vibration suppression, the synchronous vibration at 80 Hz is severe and its amplitude is up to 0.1229 g. Figure 26 illustrates the spectrum of vibration of the rotor with the proposed vibration suppression method. The synchronous vibration at 80 Hz is slight and its amplitude is 0.0064 g, which is only 5.2% of 0.1229 g, so the vibration suppression effect is remarkable.

When the speed of the rotor is less than its critical stable speed, the magnetic suspension compensation is realized by its open-loop type compensation method, and the elimination effect of the synchronous component in this case is measured. Figure 27 illustrates the spectrum of vibration of the rotor without vibration suppression. It is clear that the synchronous vibration at about 40 Hz is severe and its amplitude is large. When the open-loop-type compensation method is imposed, synchronous vibration at about 40 Hz, as illustrated in Figure 28, is slight.

From Figure 28, it is easy to find that the synchronous vibration of MSFW in the whole speed range of the rotor is suppressed effectively, so we can draw a conclusion that the vibration suppression method proposed by us for MSFW is very fit for such application as a rotor repeatedly traversing its own critical stable speed.

For the high precision balanced rotor, the synchronous component may not be the main component of vibration, and the third harmonic component may be the main component of vibration for lack of a more precision balance method. The spectrum of vibration of high precision balanced rotor for MSFW is shown in Figure 29; it is clear that the third harmonic component is the largest component with amplitude about -26 dB. After the suppression of vibration by the proposed method, the amplitude of the third harmonic component, as shown in Figure 30, has reduced to -60 dB, which is only 1.99% of its former.

6. Conclusions

Flywheel is an inertial actuator in a spacecraft attitude control system and is used to generate suitable attitude control torques for correcting spacecraft attitude deviation or adjusting to an assigned attitude. With respect to MSFW, the synchronous vibration caused by the residual unbalance of the rotor can be suppressed by active control of magnetic bearings.

The essence of the vibration caused by residual unbalance of the rotor is that the high-speed rotor does not rotate around its inertial axis. By taking advantage of the ability of a magnetic bearing to actively control the synchronous movement of the rotor, the vibration can be successfully suppressed through the elimination of the synchronous component in magnetic suspension forces. Based on the general notch filter, this method is a closed-loop style when the rotor rotates beyond its critical stable speed and is open-loop style when the speed of the rotor is less than the critical stable speed by additional displacement stiffness compensation segment – open and closed-loop control method. This method is not only stable but is also able to eliminate the n octave synchronous vibration of the rotor in the whole speed range of the rotor.

On the basis of the main parameters of MSFW, experimental results demonstrate that this method can significantly suppress the unbalance vibration caused by residual unbalance of the rotor through the magnetic suspension force compensation in the operation speeds of MSFW. This method is suitable for MSFW in that its rotor frequently traverses the critical stable speed.

Acknowledgements

The efforts of Jinji Sun, Chune Wang and Hu Liu are appreciated.

Funding

This work was supported by the National Natural Science Foundation of China (grant number 61174003).

References

Bi C, Wu DZ and Jiang Q (2005) Automatic learning control for unbalance compensation in active magnetic bearings. *IEEE Transactions on Magnetics* 41(7): 2270–2280.

Charara A, De Miras J and Caron B (1996) Nonlinear control of a magnetic levitation system without premagnetization. *IEEE Transactions on Control Systems Technology* 4: 513–523.

Johannes V, Löwis and Joachim R (2000) Adaptive inertial autocentering of a rigid rotor with unknown imbalance supported by active magnetic bearings. In: *Proceedings of the 7th International Symposium on Magnetic Bearings*, Zurich, Switzerland, August 23–25, Switzerland: International Center of Magnetic Bearings, pp. 561–566.

Kenny BH, Jansen R and Kascak P (2005) Integrated power and attitude control with two flywheels. *IEEE Transactions on Aerospace and Electronic Systems* 41(4): 1431–1448.

Li LC and Tadahiko S (2003) Compensation of rotor imbalance for precision rotation of a planar magnetic bearing rotor. *Precision Engineering* 27(3): 140–150.

Li LC, Tadahiko S and Zhang XY (2002) A simple method for rotation about the inertial axis of a rigid AMB rotor. In: *Proceedings of the 8th International Symposium on Magnetic Bearings*, Mito, Japan, August 26–28, Japan: International Center of Magnetic Bearings, pp. 405–410.

Liu B, Fang JC and Liu G (2010) Unbalance vibration control and experiment research of magnetically suspended flywheel. *Chinese Journal of Mechanical Engineering* 46: 188–194.

Peng XJ, Gao ZY and Wang YL (2006) Design of notch filter to eliminate unbalance vibration in magnetic and electrostatics bearings. *Chinese Journal of Mechanical Engineering* 42(6): 120–123.

Saito M, Fukushima K and Sato N (2006) Development of magnetic bearing wheel with inclined magnetic poles (3rd Report, *Low Disturbance Control Based on Disturbance Feedback*). *Transactions of the Japan Society of Mechanical Engineers, Part C* 72(3): 698–705.

Song B, Ma GF and Li CJ (2007) Compensation method of periodic disturbance of momentum biased satellite based on wheels. *Control Engineering of China* 14(2): 143–146.

Takeshi M (2001) Analysis of the fundamental properties of active magnetic bearing control systems by a transfer function approach. *JSME International Journal, Series C: Mechanical Systems, Machine Elements and Manufacturing* 44(2): 367–373.

Tang L and Chen YQ (2009) Mode development and adaptive unbalance vibration control of magnetic suspended system. *Acta Astronautica* 65(9–10): 1506–1514.

Wang QW and Hu G (2009) Analysis of flywheel disturbance and measuring technology. *Chinese Journal of Space Science* 29(1): 39–44.

Yin QY, Zhao JK and Dai JH (2007) A method of control inner disturbance to the reaction wheel. *Journal of Electronics & Information Technology* 29(6): 1521–1524.

Zhang XY, Tadahiko S and Li LC (2004) Precision control for rotation about estimated center of inertia of spindle supported by radial magnetic bearing. *JSME International Journal, Series C: Mechanical Systems, Machine Elements and Manufacturing* 47(1): 242–250.